THE JOURNAL OF BIOLOGICAL CHEMISTRY VOL. 285, NO. 39, pp. 30316–30327, September 24, 2010
Printed in the U.S.A.

Cardiac Restricted Overexpression of Membrane Type-1 Matrix Metalloproteinase Causes Adverse Myocardial Remodeling following Myocardial Infarction*

Received for publication, June 24, 2010 Published, JBC Papers in Press, July 19, 2010, DOI 10.1074/jbc.M110.158196

Francis G. Spinale[‡§], Rupak Mukherjee[‡], Juozas A. Zavadzkas[‡], Christine N. Koval[‡], Shenikqua Bouges[‡], Robert E. Stroud[‡], Lawrence W. Dobrucki[¶], and Albert J. Sinusas[¶1]

From the [‡]Medical University of South Carolina and the [§]Ralph H. Johnson Veterans Affairs Medical Center, Charleston, South Carolina 29425 and the [¶]Yale University School of Medicine New Haven, Connecticut 06510

The membrane type-1 matrix metalloproteinase (MT1-MMP) is a unique member of the MMP family, but induction patterns and consequences of MT1-MMP overexpression (MT1-MMPexp), in a left ventricular (LV) remodeling process such as myocardial infarction (MI), have not been explored. MT1-MMP promoter activity (murine luciferase reporter) increased 20-fold at 3 days and 50-fold at 14 days post-MI. MI was then induced in mice with cardiac restricted MT1-MMPexp ($n = 58$) and wild type (WT, $n = 60$). Post-MI survival was reduced (67% *versus* 46%, $p < 0.05$), and LV ejection fraction was lower in the post-MI MT1-MMPexp mice compared with WT (41 ± 2 *versus* $32 \pm 2\%$, $p < 0.05$). In the post-MI MT1-MMPexp mice, LV myocardial MMP activity, as assessed by radiotracer uptake, and MT1-MMP-specific proteolytic activity using a specific fluorogenic assay were both increased by 2-fold. LV collagen content was increased by nearly 2-fold in the post-MI MT1-MMPexp compared with WT. Using a validated fluorogenic construct, it was discovered that MT1-MMP proteolytically processed the pro-fibrotic molecule, latency-associated transforming growth factor-1 binding protein (LTBP-1), and MT1-MMP-specific LTBP-1 proteolytic activity was increased by 4-fold in the post-MI MT1-MMPexp group. Early and persistent MT1-MMP promoter activity occurred post-MI, and increased myocardial MT1-MMP levels resulted in poor survival, worsening of LV function, and significant fibrosis. A molecular mechanism for the adverse LV matrix remodeling with MT1-MMP induction is increased processing of pro-fibrotic signaling molecules. Thus, a proteolytically diverse portfolio exists for MT1-MMP within the myocardium and likely plays a mechanistic role in adverse LV remodeling.

The expression of a family of matrix proteases, termed the matrix metalloproteinases (MMPs),[2] have been demonstrated to occur in patients and animals with cardiovascular disease particularly in the context of adverse left ventricular (LV) remodeling such as myocardial infarction (MI) (1–4). Using transgenic and pharmacological approaches, a cause-effect relationship has been demonstrated between the induction of MMPs and adverse LV remodeling (4–9). However, there are a large number of MMP types that are expressed within the myocardium, and a unique functionality likely exists for each of these MMP types with respect to the LV-remodeling process. Thus, the identification of how specific MMP types may affect LV remodeling such as that which occurs following MI, would provide critical insight into developing more specific therapeutic strategies to interrupt this process. One of the more unique MMP types, which has been identified within the human myocardium, is the membrane type MMPs (MT-MMPs) of which the MT1-MMP subtype has been the most studied (8, 10–16). As the name implies, MT1-MMP is a transmembrane protein with a diversity of biological functions that include: 1) degradation of a spectrum of matrix structural proteins, 2) proteolytic processing of biologically active molecules such as growth factors and cytokines, and 3) activation of other MMPs. A significant increase in the myocardial levels of MT1-MMP has been identified in patients with LV failure, and the relative magnitude of this increase was greater than that of any other MMP sub-class (6). In animal models, MT1-MMP myocardial levels are increased early and appear sustained in the post-MI period coincident with adverse LV remodeling (3, 10). However, a direct relationship between increased myocardial levels of MT1-MMP and adverse LV remodeling has not been established. Accordingly, the central hypothesis of this study was that a persistent induction of MT1-MMP occurs following MI, and that selectively increasing MT1-MMP levels within the myocardial compartment would adversely affect LV remodeling post-MI.

MATERIALS AND METHODS

Overview and Rationale—The first set of experiments were performed to directly quantify MT1-MMP promoter activity *in vivo* following MI induction. This was accomplished through left coronary artery ligation in a transgenic mouse model in which the full-length human MT1-MMP promoter-reporter had been inserted and performing serial studies post-MI. A second set of experiments was performed whereby MI was induced in mice with cardiac restricted overexpression of MT1-

* This work was supported, in whole or in part, by National Institutes of Health Grants HL057952, HL059165, and HL078825. This work was also supported by a Merit Award from the Veterans Affairs Health Administration.

[1] To whom correspondence should be addressed: Cardiothoracic Surgery, Room 625, 770 MUSC Complex, 114 Doughty St., Charleston, SC 29425. Tel.: 843-876-5186; Fax; 843-876-5187; E-mail: wilburnm@musc.edu.

[2] The abbreviations used are: MMP, matrix metalloproteinase; LV, left ventricular; MI, myocardial infarction; LTBP-1, latency-associated transforming growth factor-1 binding protein; %ID, percentage of injected dose; MOPS, 4-morpholinepropanesulfonic acid; ANOVA, analysis of variance; rtPCR, real-time PCR.

MMP (MT1-MMPexp). Survival, LV function and geometry, MT1-MMP levels and specific activity, and myocardial collagen content were then determined and compared with wild type (WT) littermates. Because MT1-MMP is now recognized as a predominant pathway by which the pro-form of MMP-2 (proMMP-2) is proteolytically processed to active MMP-2 (12–14), the relative levels of these different MMP-2 forms were assessed by zymography (3, 5–7, 9). One of the initial critical steps for matrix-bound transforming growth factor (TGF) to become a competent pro-fibrotic signaling molecule, is through the proteolytic release by the TGF latency binding protein, LTBP-1 (17, 18). A cell-based study demonstrated that MT1-MMP influenced TGF signaling by proteolytically processing LTBP-1 (19). This pathway was more carefully examined in the present study through the development of an MT1-MMP-specific LTBP-1 proteolytic assay and measuring indices of TGF signaling following MI.

MT1-MMP Promoter Activity—A transgenic MT1-MMP reporter line on the FVB murine background was established by using the human genomic MT1-MMP fragment extending from −3364 bp relative to the transcriptional start site to the first intron. The generalized approach for insertion of MMP promoter-reporter constructs has been published previously (21). The MT1-MMP coding sequence start codon was cloned into p1.2 upstream from the SV40 polyadenylation site. The firefly luciferase gene (*luc*, 550-amino acid ORF) was then isolated and ligated between the MT1-MMP promoter and the SV40 polyadenylation sequence to generate the final construct: MT1-MMP3364/luc. Five independent MT1-MMP reporter lines were established and backcrossed, and then utilized in the MI studies. At designated time points, the LV was isolated, and separated into MI and remote regions, RNA extracted and samples prepared for PCR as described in detail in a subsequent section. Luciferase and 18 S mRNA levels were then determined.

MT1-MMP Overexpression—The transgenic construct expressing the human MT1-MMP coding sequence under control of the cardiac restricted murine α-myosin heavy chain promoter (MHC) was generated by ligating a 600-bp fragment of the human growth hormone polyadenylation sequence (hGHpA) to the 3′-end of the hMT1-MMP cDNA. This fragment (hMT1-MMP-hGHpA) was then inserted into the pBSII-SK+ plasmid containing the murine MHC promoter (5.5 kb) described previously (20). The 11.7-kp plasmid was then restriction digested with Not1, and an 8.8-kb DNA fragment (MHC-hMT1-MMP-hGHpA) was isolated, purified, and injected into the pronuclei of fertilized FVB mouse embryos (University of Cincinnati Transgenic Mouse Core Facility). Transgenic mice possessing the construct were identified by PCR from tail-snip DNA. Routine genotyping was performed by PCR using primers for hMT1-MMP (forward, 5′-AAGCCT-GGCTACAGCAAT-3′; and reverse, 5′-GGCCTGCTTCT-CATGG-3′). Three independent lines of MT1-MMPexp mice were developed and following backcrossing and stable breeding patterns, ~50% from each litter were MT1-MMPexp-positive (22). Further confirmation studies for the full-length human MT1-MMP were performed by quantifying mRNA and protein levels as described in a subsequent section. The MT1-MMPexp-negative mice were used as referent, WT sibling controls. The MT1-MMPexp mice displayed no obvious phenotypic abnormalities. MT1-MMPexp and WT mice were maintained until 3 months of age and then randomized to undergo LV functional assessment and myocardial sampling or to undergo surgically induced MI.

Myocardial Infarction—Mice were anesthetized by isoflurane (2%, the LV visualized, and the main left coronary artery ligated (8.0 Neurilon, Ethicon, K801) (9, 21, 23). The intra-operative mortality (first 24 h) was 15% and similar between groups. The mice were followed for 14 days post-MI at which time a second echocardiogram was performed and the LV harvested for histomorphometry and MT1-MMP measurements. For *in situ* imaging in the MT1-MMP reporter line, the mice were anesthetized, an intraperitoneal injection of luciferin (5 mg, Promega) was performed, the heart harvested, and bioluminescent signals collected by an IVIS 200 system (Xenogen, Alameda, CA). The LV was then processed for biochemistry and histochemistry. All animals were treated and cared for in accordance with the National Institutes of Health "Guide for the Care and Use of Laboratory Animals" (National Research Council, Washington, 1996) and under an approved Medical University of South Carolina Institutional Animal Care and Use Committee protocol (ARC# 2389).

LV Geometry and Function—Transthoracic echocardiography was performed to measure LV geometry and function (8, 9, 22, 23). Two-dimensional M-mode echocardiographic recordings were obtained using a 40-MHz scanning head with a spatial resolution of 30 μm (Vevo 660, VisualSonics, Toronto). Using long axis views, LV end-diastolic volume, posterior wall thickness, ejection fraction, and mass were computed. Then, the mice were positioned on a feedback temperature-controlled operating table (Vestavia Scientific, Birmingham, AL) and maintained with 2% isoflurane anesthesia. At 14 days post-MI, echocardiograms were repeated in identical fashion. Following the final set of measurements, and under a full surgical plane of anesthesia (isoflurane 4%), the LV was removed and then processed for histochemistry or biochemical analysis.

MMP Targeted Radiotracer Activity Studies—An *in vivo* index of total MMP activity was determined in a subset of WT and MT1-MMPexp mice using a radiotracer approach described in detail by this laboratory previously (23). For these studies, the mice were anesthetized as described in the previous section, and the external jugular vein was cannulated. The MMP targeted radiotracer ^{99m}Tc-RP805, which binds with high affinity to all active MMPs, was then injected (1.32 ± 0.43 mCi). Then, the conventional myocardial perfusion radiotracer, ^{201}Tl chloride was injected (0.22 ± 0.09 mCi). Fifteen minutes after the injections, the mice were then deeply anesthetized (4% isoflurane), and the LV was harvested and cut into 2-mm slices parallel to the LV short axis. Each slice was then cut into four segments (anterior, lateral, posterior, and septal) for gamma well counting (Cobra Packard) of ^{201}Tl and ^{99m}Tc activity. Raw counts were corrected for spill-up/spill-down, background, decay, and weight (mCi/g). ^{99m}Tc-RP805 activity in each myocardial segment was then calculated as the percentage of injected dose (%ID). The calculated %ID was computed by dividing corrected tissue counts (mCi/g) by the decay-cor-

rected injected dose (mCi) and expressed in %ID per gram of tissue.

Histomorphometry and Immunohistochemistry—For the histomorphometry studies, sections (5 μm) were stained with hematoxylin and eosin for measurement of MI size using computer-assisted planimetry (Sigma Scan, Media Cybernetics). LV sections were stained with picro-sirius red for fibrillar collagen, and the percent area of collagen within the remote and MI regions of the LV computed (5, 9, 22). For the MT1-MMP promoter studies, LV frozen sections (7 μm) were incubated overnight with a luciferase antisera (SC32896, 1:100), washed in PBS and incubated with a secondary antisera (Molecular Probes, A11008, 1:250) for 30 min followed the nuclear stain To-Pro-3 (Molecular Probes, T3605, 1:750). For MT1-MMP localization, the LV sections were first incubated with an MT1-MMP antisera (AB815, 1:250) overnight at 4 °C, washed in PBS, and incubated with a secondary antisera (Molecular Probes, A11008, 1:250) for 30 min, washed, and incubated with Phalloidin (Molecular Probes, A22283, 1:40) for 30 min, washed, incubated with To-Pro-3 (Molecular Probes, T3605, 1:750) for 10 min. The stained LV sections were washed, coverslips were added (Vectashield Mounting Media), and sections were examined by confocal microscopy (Zeiss LSM 510) where the triple stained images were sequentially examined with excitation/emission wavelengths of 495/524, 546/570, and 642/661 nm.

Myocardial MMPs—Substrate zymography was performed to assess the relative content of the gelatinases MMP-2 and MMP-9 (2–9). A positive control was utilized in all zymography measurements (2 μg, MMP-2/9 S.E.-244/237, BIOMOL). Immunoblotting was performed for MT1-MMP (AB8221, Millipore, 0.8 μg/ml). For the MT1-MMP immunoblotting and activity assays, LV myocardium was homogenized in ice-cold 250 mM sucrose/20 mM MOPS buffer. The homogenate was centrifuged (100,000 $\times$ *g*, 1 h), and the membrane fraction was re-suspended in buffer. A positive control for MT1-MMP (CC1043, 300 ng) was included in every assay.

MT1-MMP and LTBP-1 mRNA Measurements—LV myocardial homogenates were subjected to RNA extraction (RNeasy Fibrous Tissue Mini Kit, Qiagen, Valencia, CA), and the quantity and quality of the RNA were determined (Experion Automated Electrophoresis System, Bio-Rad Laboratories, Hercules, CA). RNA (1 μg) was reverse transcribed to generate cDNA (iScript cDNA Synthesis Kit, Bio-Rad). The cDNA was amplified with gene-specific primer/probe sets (TaqMan Universal PCR Master Mix: catalog no. 4364321, Applied Biosystems, Foster City, CA) using single-color Real-Time PCR (rtPCR, MyiQ, Bio-Rad). The specific TaqMan primer/probe sets (Applied Biosystems) were human MT1-MMP (catalog no. Hs0000237119_m1), mouse MT1-MMP (catalog no. Mm01318965_m1), mouse LTBP-1 (catalog no. Mm0049825_m1), and 18 S rRNA (catalog no. 4333760F). Negative controls were run to verify the absence of genomic DNA contamination (reverse transcription control), and the absence of overall DNA contamination in the PCR system and working environment (template control). The rtPCR fluorescence signal was converted to cycle times (C_t), normalized to the 18 S signal, and final expression levels were determined as a function of total RNA concentrations.

MT1-MMP Activity Assay—LV myocardial membrane extracts (50 μg) were prepared and incubated with a specific MT1-MMP fluorogenic substrate (MMP-14 Substrate I, catalog no. 444258, Calbiochem) described previously (10). The LV myocardial extracts were incubated (37 °C) in the presence and absence of the MT1-MMP substrate, and excitation/emission were recorded (328/400, FluoStar Galaxy, BMG Labtech Inc., Durham, NC) continuously for up to 20 h. Increasing concentrations of a recombinant active MT1-MMP construct (MT1-MMP Catalytic Domain, catalog no. 475935, Calbiochem 8–125 ng/ml) with a known catalytic activity, resulted in a linear relationship with respect to fluorescence emission ($y = 343x$, $r^2 = 0.98$, $p = 0.001$).

LTBP-1 Proteolytic Processing by MT1-MMP—The full-length sequence for LTBP-1 (NCBI, AAI30290.1) was first examined for MT1-MMP substrate binding/cleavage sites as described previously (24). From these initial mapping studies, a series of peptide mimics were next assessed for MT1-MMP proteolytic specificity. Three potential peptides were identified: A176 (SGRSENIRTA), A42 (SGRIGFLRTA), and B175A (SGAAMHMYTA). The peptides were aligned to each individual sequence of interest to identify potential binding/cleavage sites using the ClustalW+ alignment algorithm with the BLOSSUM scoring matrix.[3] Sequences demonstrating positive peptide alignment were analyzed for domain structure using the Simple Modular Architecture Research Tool to assess putative cleavage sites. Peptide A176 demonstrated a high concordance with LTBP-1 and significant alignment for MT1-MMP-specific cleavage. This peptide sequence in a caged fluorogenic construct (AnaSpec Inc., Fremont, CA, newly assigned peptide name: SCJJ-1) with a certified HPLC purity of >98% was then synthesized. Using the approaches described previously (10, 22), and a specific excitation/emission wavelength (340/485 nm), 15 μM LTBP-1 was exposed to increasing concentrations of the MT1-MMP catalytic domain. A clear fluorescent signal was detected with increasing concentrations of MT1-MMP, which was highly linear. Co-incubation with the MT1-MMP-selective inhibitor (0007258, 5 pM), the global MMP inhibitor (BB94, 1 μM) or MT1-MMP blocking antibody (1 μg/ml, AB8101) extinguished all fluorescent activity. LV myocardial extracts were subsequently incubated (37 °C) in the presence and absence of the MT1-MMP-neutralizing antisera, and fluorescence emission were recorded for up to 20 h. For both activity assays, utilizing known concentrations of the MT1-MMP catalytic domain and the fixed periods of incubation, an absolute catalytic activity for MT1-MMP- and LTBP-1-mediated proteolysis could be computed.

To more carefully localize the sites of MT1-MMP-mediated LBTP-1 proteolysis, parallel frozen LV sections (7 μm) were immersed with 100 μM of the LTBP-1 substrate or reaction buffer only and placed on a thermostatically controlled stage (37° C) and imaged by confocal microscopy using the system described in the previous section. Time lapsed digital images were acquired every 20 min (405/430–470 nm) using

[3] ClustalW+ alignment algorithm with the BLOSSUM scoring matrix (SeqWeb (v3.1.2) interface to the Genetic Computer Group, Wisconsin Package (V10.3) analysis software, Accelrys, Inc., San Diego, CA).

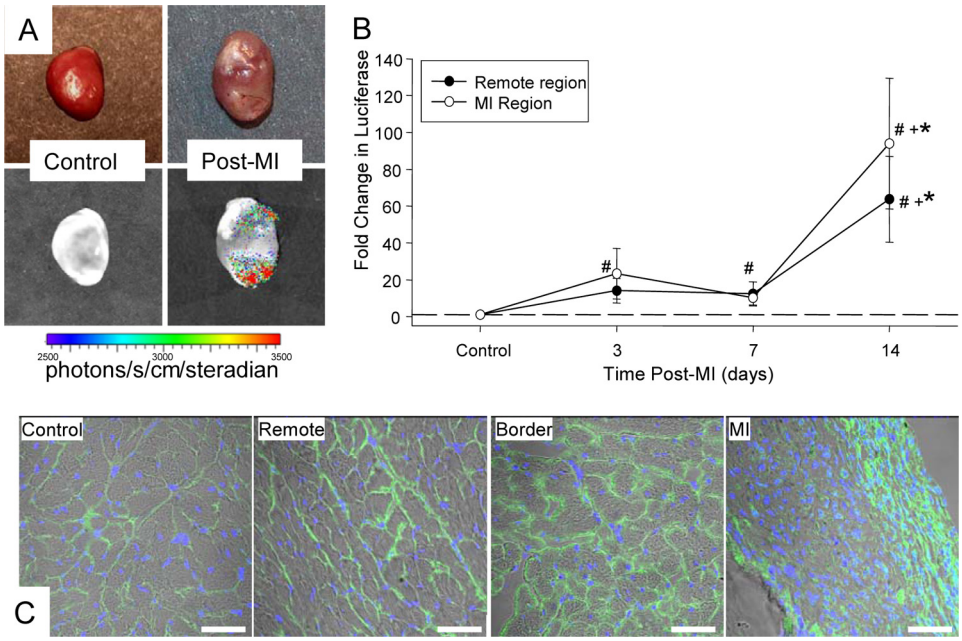

FIGURE 1. **MT1-MMP promoter activity was assessed using a transgenic construct whereby the human MT1-MMP promoter region ligated to the luciferase gene was permanently inserted.** *A*, following injection of luciferin, bioluminescent imaging of extracted hearts was performed. Representative standard field photographs are shown at the *top*, whereas registered and digitized images of whole bioluminescent scans are shown at the *bottom*. Although an absence of a bioluminescent signal was detected in control hearts, a strong luciferin bioluminescent signal could be readily detected by 14 days post-MI, indicative of increased MT1-MMP promoter activity, within the MI and remote regions. *B*, luciferase mRNA levels were determined in control and in the MI and remote regions at 3, 7, and 14 days post-MI (n = 5–6/time point). A significant increase in luciferase levels, indicative of increased MT1-MMP promoter activity, occurred within the MI region by 3 days post-MI and was significantly increased within the MI and remote regions by 14 days post-MI. *C*, immunohistochemical localization for luciferase was performed in control and post-MI sections. A weak, but positive signal for luciferase (*green*) was observed in control sections, indicative of basal MT1-MMP promoter activity, but was robustly increased in 14-day post-MI sections within the MI, border, and remote regions. DNA staining (*purple*/*blue*) provided identification of nuclei. Luciferase staining was predominantly localized to the interstitial space, suggestive that the predominant induction of MT1-MMP was within myocardial fibroblasts. (*Scale* = 20 μm.)

a high voltage gain (481) and a low voltage gain (375) setting. Isochronal difference interference contrast images were also obtained.

LTBP-1 Processing, TGF-R1, and Smad-2—In light of the fact that LTBP-1 is initially a high molecular weight protein, which is subsequently proteolytically processed to low molecular weights (19), LV extracts (20 μg of total protein) were loaded onto 3–8% Tris acetate gels (EA03785, Invitrogen, Carlsbad, CA). The LV extracts were rigidly maintained in a protease inhibitory mixture (150 mM EDTA, 1 mM PMSF, 1 mM aprotinin, 1 mg/ml leupeptin, 1 mg/ml pepstatin). Immunoblotting was performed for LTBP-1 (SC28133, 1:200). In all of these studies, a positive control for LTBP-1 (30 μg, 3611-RF whole cell lysate, catalog no. sc-2215, Santa Cruz Biotechnology, Santa Cruz, CA) was utilized. Next, relative levels of the TGF-R1 were determined in LV extracts by immunoblotting (sc-398, 1:200). Finally, LV myocardial levels for a common intracellular convergence point of the TGF receptor transduction pathway, Smad-2 (17, 18). For these studies, immunoblotting was first performed for total Smad-2, the membranes were stripped and re-probed for phosphorylated Smad-2 (Cell Signaling, #3102/3104, respectively, 1:1000).

Data Analysis—LV function and geometry were compared between the referent control and aging groups using an analysis of variance (ANOVA), and pairwise comparisons were performed by a Bonferroni adjusted t test. The zymographic/immunoreactive signals were analyzed using densitometric methods (Gel Pro Analyzer, Media Cybernetics) to obtain two-dimensional integrated optical density values. The integrated optical density values were then computed as a percent of control values where the control values were set to 100%, and comparisons were performed by a separate t test. For the MMP immunoassays and mRNA measurements, a Winsorized mean was utilized if extreme values existed in the data set. Between-group differences in these values were compared using ANOVA followed by Bonferroni adjusted t test. For the morphometric data (percent collagen), the data were first confirmed to conform to a Gaussian distribution, subjected to ANOVA, and finally to Tukey's test for mean separation. For the survival portion of the study, survival curves were constructed utilizing Kaplan-Meier probability estimates and 14-day post-MI survival compared utilizing a Chi-Square analysis. Values of $p < 0.05$ were considered statistically significant. All statistical procedures were performed using the STATA statistical software package (Statacorp, College Station, TX). Results are presented as means ± S.E. Final sample sizes for each protocol/experiment are indicated in the figure legends.

RESULTS

Myocardial MT1-MMP Promoter Activity and MI

MT1-MMP promoter activity was assessed using a transgenic construct whereby the human MT1-MMP promoter region ligated to the luciferase gene was permanently inserted. While a bioluminescent signal was not detected in non-MI hearts, a strong luciferin signal could be readily detected at 14 days post-MI, indicative of increased MT1-MMP promoter activity, within the MI and remote regions (Fig. 1). Temporal profiling of MT1-MMP promoter activity through measuring luciferase mRNA levels is shown in Fig. 1, where levels increased within the MI region by 3 days post-MI, and were significantly increased within the MI and remote regions by 14 days post-MI (Fig. 1). Immunohistochemical localization for luciferase was performed in control and post-MI sections (Fig. 1). A weak, but positive signal for luciferase was observed in control sections, indicative of

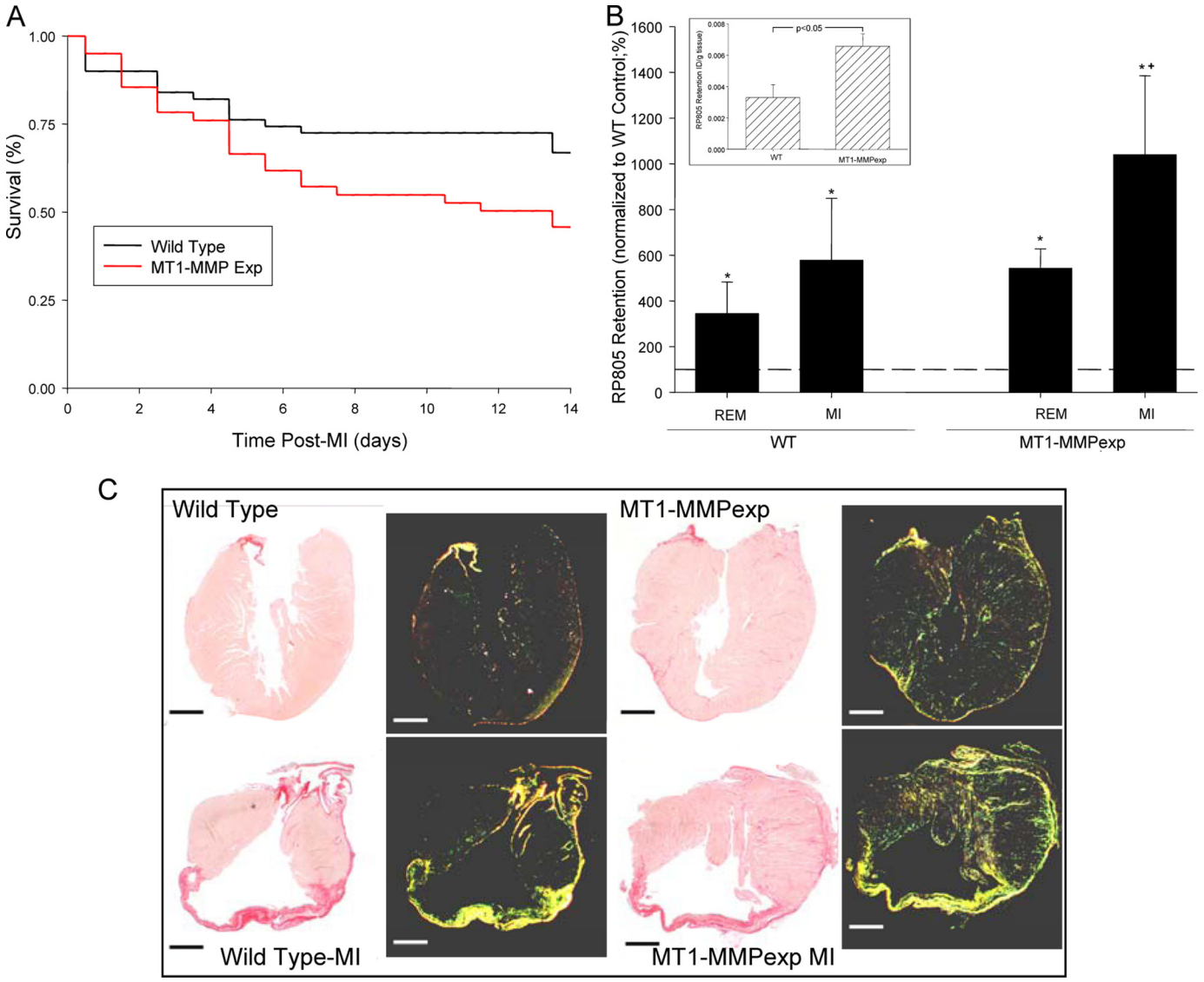

FIGURE 2. *A*, post-MI 14-day survival was significantly lower in the MT1-MMPexp mice following MI when compared with WT mice ($\chi^2 = 7.6$, $p = 0.006$). *B*, a relative index of total *in vivo* MMP activity was determined using an MMP radiotracer ^{99m}Tc-RP805 (22). *Inset*, total myocardial MMP radiotracer retention was significantly higher in referent control MT1-MMPexp when compared with WT mice ($n = 5$/group). At 14 days post-MI ($n = 6$/group), increased MMP radiotracer uptake occurred within both the remote and MI regions, but was nearly 2-fold higher within the MI region in the MT1-MMPexp group ($n = 6$) (*, $p < 0.05$ *versus* WT non-MI; $^{+}$, $p < 0.05$ *versus* WT remote). *C*, long axis LV sections were stained with picro-sirius and viewed under bright field (*left panels*) as well as polarized light (*right panels*) taken from WT and MT1-MMPexp mice. Increased collagen staining was observed in the MT1-MMPexp mice. At 14 days post-MI, significant LV enlargement was observed in both groups, but substantially higher myocardial collagen was observed within remote viable myocardium in the MT1-MMPexp mice. (*Scale* = 1 mm.)

basal MT1-MMP promoter activity, but was robustly increased in 14-day post-MI sections within the MI, border, and remote regions.

Cardiac Overexpression of MT1-MMP and MI

Survival and LV Function and Geometry—A total of 60 WT mice and 58 MT1-MMP mice underwent surgically induced MI and survived the initial 24-h post-operative period. The 14-day post-MI survival was significantly worse in the MT1-MMPexp mice when compared with age-matched WT mice (Fig. 2). Post-mortem analysis revealed that ~10% of the deaths were due to myocardial rupture at the LV apical region, 50% were due to occult cardiac decompensation as evidenced by significant serous fluid accumulation within the thoracic space, and 40% revealed no significant transudate or serosanginuous fluid in the thoracic space and, therefore, the deaths were presumed to be of an arrhythmic origin. LV function and geometry by echocardiography were assessed in the mice surviving at 14 days in the WT group ($n = 37$) and the MT1-MMPexp group ($n = 21$) and were compared with age-matched, sham-referent WT and MT1-MMPexp groups ($n = 32$ and $n = 20$, respectively). Heart rates during this study period were equivalent across all groups (range 480–500 bpm). In the WT controls, LV end-diastolic volume was similar between the WT and MT1-MMPexp groups (44 ± 2, 43 ± 2 μl, respectively). However, LV ejection fraction was lower in the MT1-MMPexp group compared with WT (56 ± 2, $65 \pm 1\%$, $p = 0.03$, respectively). At 14 days post-MI, LV end-diastolic volume increased to a similar degree from

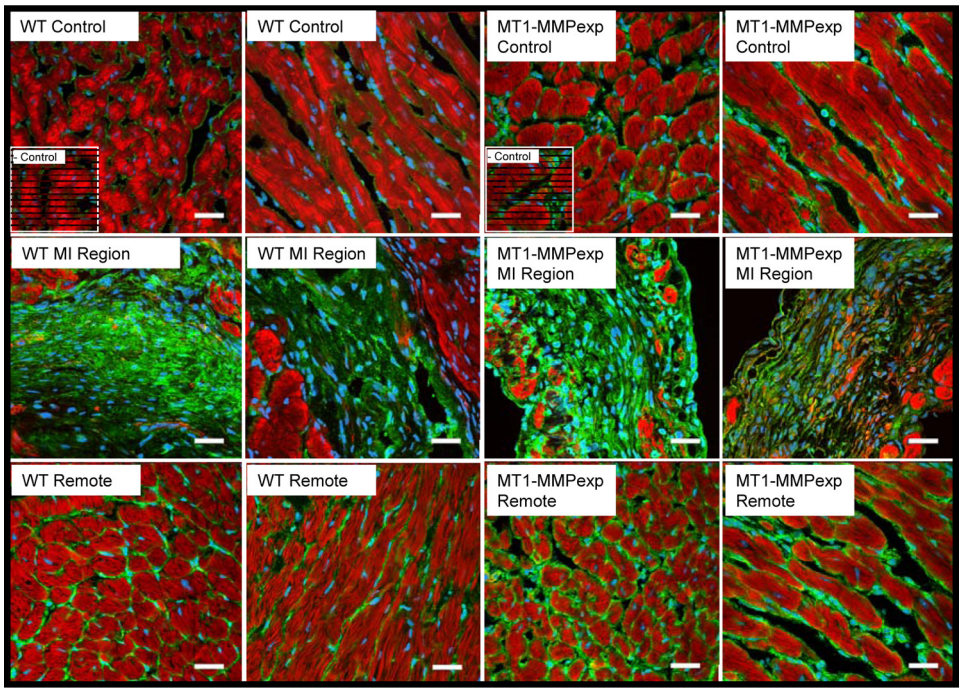

FIGURE 3. **Representative LV sections in which MT1-MMP was localized by immunofluorescence using confocal microscopy in WT and MT1-MMPexp mice.** *Green* fluorescence represents MT1-MMP, *red* fluorescence is indicative of rhodamine-phalloidin, and the *blue stain* is indicative of nuclei. Increased relative abundance and staining intensity for MT1-MMP was observed along the myocyte-matrix interface in LV sections taken MT1-MMPexp mice. At 14 days post-MI, a robust increase in MT1-MMP staining was observed within the MI region for both WT and MT1-MMPexp mice. However, in the MT1-MMPexp mice, a more robust and greater staining pattern was clearly observed within the remote regions. (*Scale* = 20 μm.)

respective control values in both the WT and MT1-MMPexp groups (75 ± 3, 77 ± 4 μl, $p < 0.05$). LV ejection fraction fell in the WT-MI group (41 ± 2%, $p < 0.002$) and was reduced to a greater degree in the MT1-MMPexp group at 14 days post MI (32 ± 2%, both $p < 0.05$). At 14 days post-MI, LV mass was similar between the WT and MT1-MMPexp groups (4.7 ± 0.2, 5.0 ± 0.2 mg/g, respectively). Thus, in this post-MI period, reduced survival and more severe systolic dysfunction occurred in the MT1-MMPexp group.

MMP Activity in Vivo—A relative index of total in vivo MMP activity was determined in a subset of mice at 14 days post-MI using a previously described and validated MMP radiotracer ^{99m}Tc-RP805 (Fig. 2) (23). Total myocardial MMP radiotracer retention, indicative of total MMP activity, was higher in referent control MT1-MMPexp when compared with WT mice. At 14 days post-MI, increased MMP radiotracer uptake occurred within both the remote and MI regions, but was nearly 2-fold higher within the MI region in the MT1-MMPexp group.

MI Size and Collagen Content—Computed MI size was equivalent between the WT and MT1-MMP groups (35 ± 4 and 38 ± 7%, respectively). Long axis LV sections were stained with picro-sirius, and representative photomicrographs are shown in Fig. 2. An observable increase in LV myocardial collagen occurred in the MT1-MMPexp mice under control conditions as well as following MI. In the referent control groups, relative fibrillar collagen was increased within the LV free wall in the MT1-MMPexp group when compared with WT (1.71 ± 0.14, 0.56 ± 0.12%, $p = 0.006$). At 14 days post-MI, fibrillar collagen was increased from referent control values within the MI region in both the WT and MT1-MMPexp groups (13.62 ± 0.82, 24.31 ± 3.71%, $p = 0.005$, respectively) but was higher in the MT1-MMPexp group ($p = 0.008$). Within the remote region, fibrillar collagen was also increased from referent controls (1.71 ± 0.30, 4.97 ± 0.78%, $p < 0.05$, respectively) and was significantly higher in the MT1-MMPexp group ($p = 0.004$). Thus, MT1-MMPexp was associated with a nearly 2-fold increase in fibrillar collagen content under referent control conditions and following MI.

MT1-MMP Distribution, Content, mRNA Levels, and Activity Post-MI—Representative LV sections in which MT1-MMP was localized by immunofluorescence using confocal microscopy are shown in Fig. 3. Increased relative abundance and staining intensity for MT1-MMP was observed along the myocyte-matrix interface in LV sections taken MT1-MMPexp mice. At 14 days post-MI, a robust increase in MT1-MMP staining was observed within the MI region for both WT and MT1-MMPexp mice. However, in the MT1-MMPexp mice, a more robust and greater staining pattern was clearly observed within the remote regions. LV myocardial membrane extracts were subjected to MT1-MMP immunoblotting, and the results are summarized in Fig. 4. Total MT1-MMP myocardial levels, which included the full-length active and truncated active forms (51–55 kDa) (12–14), significantly increased following MI in the WT group. Total MT1-MMP levels were increased in both of the MT1-MMPexp groups, where total MT1-MMP levels were increased by over 2-fold in the post-MI MT1-MMPexp group. The relative mRNA levels for both mouse and human MT1-MMP were determined by rtPCR and are summarized in Fig. 5. The relative mRNA levels for mouse MT1-MMP increased in the WT group at 14 days post-MI, whereas the relative levels for mouse MT1-MMP decreased in both MT1-MMPexp groups. A robust level of human MT1-MMP mRNA was detected in both MT1-MMPexp groups and, as expected, not detected in the WT groups. LV myocardial extracts were subjected to gelatin zymography (Fig. 4), which provides a measure of relative MMP-9 and MMP-2 levels. Relative MMP-9 levels were increased in the post-MI groups, as were total MMP-2 levels. Molecular weight fractionation of the MMP-2 zymographic bands revealed a pronounced increase in the active form of MMP-2 (64 kDa) in the MT1-MMPexp groups, which was further increased post-MI. Because MT1-MMP is a fundamental mechanism for proteolytic cleavage of proMMP-2 to active MMP-2 (12–15), this provided indirect evidence for increased MT1-MMP activity in the MT1-

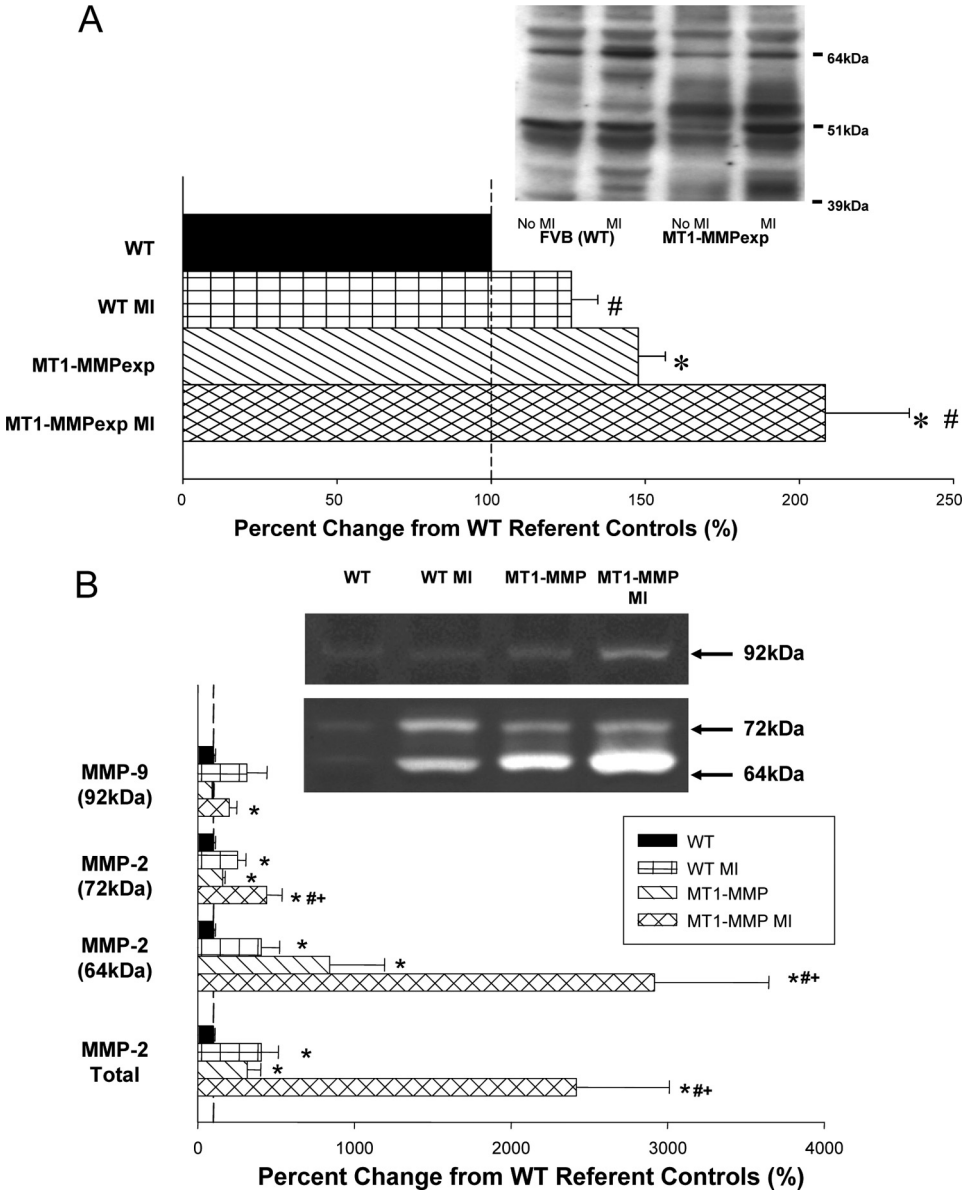

FIGURE 4. *A*, LV myocardial membrane extracts from wild type (*WT*), WT at 14 days post-MI, MT1-MMP overexpression (*MT1-MMPexp*), and at 14 days post-MI were subjected to MT1-MMP immunoblotting ($n = 10$/group). Total MT1-MMP myocardial levels, which includes the full-length and truncated active forms (51–55 kDa) significantly increased following MI. As expected, MT1-MMP total levels were increased in the MT1-MMPexp groups, and were increased by ~2-fold following MI. *B*, crude LV myocardial extracts were subjected to gelatin zymography, which provides a measure of relative MMP-9 and MMP-2 levels. Relative MMP-9 levels were increased in the post-MI groups, as were total MMP-2 levels. Molecular weight fractionation of the MMP-2 zymographic bands revealed a pronounced increase in the active form of MMP-2 (64 kDa) in the MT1-MMPexp groups, which was further increased post-MI. (*, $p < 0.05$ *versus* WT non-MI; $^{\#}$, *versus* MT1-MMPexp non-MI; $^{+}$, $p < 0.05$ *versus* WT MI.)

MMPexp groups. Accordingly, LV myocardial membrane extracts were then utilized to directly measure MT1-MMP catalytic activity using a calibrated and validated fluorogenic substrate (Fig. 6) (10). Myocardial MT1-MMP activity in LV myocardial extracts was assessed continuously for specific fluorescent emission over a 20-h period, and through this approach, a clearly heightened MT1-MMP activity was observed in both MT1-MMPexp groups. Although MT1-MMP activity was increased at 14 days post-MI in the WT group, MT1-MMP activity was increased by over 2-fold in the respective MT1-MMPexp group. Thus, the MT1-MMPexp construct yielded a robust increase in the full-length MT1-MMP, which could be demonstrated within the myocardium, was proteolytically competent, and increased by nearly 2-fold following MI.

MT1-MMP and Pro-fibrotic Signaling Post-MI—Because MT1-MMPexp was associated with a heightened pro-fibrotic response, then critical components of the TGF signaling cascade were examined, which included MT1-MMP-mediated LTBP-1 proteolysis, TGF receptor density, and relative content and phosphorylation of a common intracellular convergence point, Smad-2 (17, 18). LV myocardial extracts were used to measure MT1-MMP-specific proteolysis using a specific LTBP-1 fluorogenic substrate (Fig. 6). Through continuous monitoring of fluorescence emission over a 20-h period, which would be reflective of MT1-MMP-mediated LTBP-1 proteolytic activity, significantly higher levels were observed in the MT1-MMPexp groups when compared with WT and was further increased following MI. Next, immunoreactive bands corresponding to the full-length and proteolytically processed forms of LTBP-1 were measured (Fig. 6). Densitometry demonstrated a relative reduction in the full-length LTBP-1 in the MT1-MMPexp group compared with WT controls, which fell further in the MT1-MMPexp group following MI. In contrast, low molecular weight forms of LTBP-1 increased in the MT1-MMPexp groups. Finally, to provide direct demonstration that MT1-MMP-mediated LTBP-1 proteolysis occurred *in situ*, LV frozen sections were incubated with the LTBP-1 substrate, and localized fluorescent emission was visualized over a 6-h period (Fig. 6). A significant and time-dependent fluorescent signal was observed, indicative of MT1-MMP-specific LTBP-1 proteolysis along the border zone and MI regions. Because this fluorescent signal was detected within the MI region as well as in viable myocardium, this would indicate that MT1-MMP expression in both fibroblasts and myocytes can contribute to LTBP-1 proteolysis following MI. Finally, LTBP-1 mRNA levels were determined by rtPCR (Fig. 5), which demonstrated a relative reduction in the MT1-MMPexp groups. Through immunoblotting,

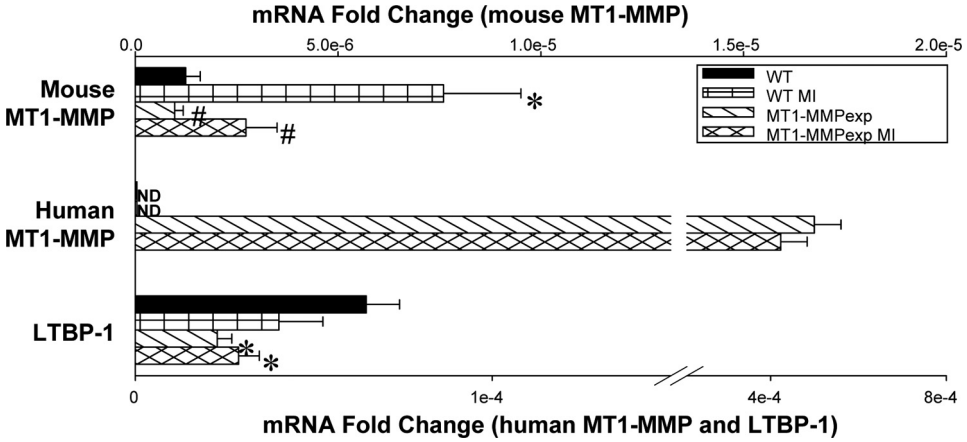

FIGURE 5. **The relative mRNA levels for the endogenous mouse MT1-MMP, human MT1-MMP, and the mouse LTBP-1 were computed using rtPCR from myocardial RNA extracted from wild type (*WT*), WT at 14 days post MI, MT1-MMP overexpression (*MT1-MMPexp*), and at 14 days post-MI ($n = 10$/group).** The levels were normalized to 18 S mRNA, and the -fold change was computed from the relative C_t values obtained for the mRNA of interest and 18 S mRNA. In the post-MI WT group, a significant increase in the endogenous mouse MT1-MMP mRNA levels occurred, whereas these levels were reduced in the MT1-MMPexp groups. As expected, a robust signal for human MT1-MMP mRNA was obtained in both MT1-MMPexp groups and not detected (*ND*) in both WT groups. LTBP-1 mRNA levels were reduced in both MT1-MMPexp groups when compared with WT values. (*, $p < 0.05$ *versus* WT non-MI; $^{+}$, *versus* MT1-MMPexp non-MI; $^{\#}$, $p < 0.05$ *versus* WT MI.)

the total levels of TGF receptor-1 were significantly increased in the MT1-MMP post-MI group (Fig. 7). Total phosphorylated Smad-2 was increased to the greatest extent in the post-MI MT1-MMP group. Thus, MT1-MMPexp resulted in greater proteolytic activity and proteolytic processing of LTBP-1, increased TGF receptor density, and heightened phosphorylation of Smad-2.

DISCUSSION

Changes in the expression and activity of the large family of MMPs have been well documented in animal models and in clinical studies of LV remodeling (1–10). Moreover, transgenic models and pharmacological MMP inhibition studies have demonstrated a cause-effect relation between MMP activity and adverse LV remodeling; particularly post-myocardial infarction (MI) (2, 4, 9). However, the expression patterns and functionality of the different classes and subtypes of MMPs are unique and therefore may have disparate effects on post-MI remodeling. One class of MMPs with a diverse substrate portfolio as well as unique functional aspects is the membrane-type MMPs (MT-MMPs) of which MT1-MMP can be considered prototypical (12–16). Using transgenic constructs, which provided for direct measurement of MT1-MMP promoter activity as well as cardiac restricted overexpression of MT1-MMP (MT1-MMPexp), the unique and important findings of the present study were 3-fold. First, increased MT1-MMP promoter activity occurs early, is sustained in the post-MI period, and occurs within both the MI and remote myocardial regions. Second, MT1-MMPexp reduced post-MI survival, worsened LV systolic function, and amplified a pro-fibrotic response in both the MI and remote myocardium. Third, net MMP proteolytic activity was induced by MT1-MMPexp, increased proteolytic processing of LTBP-1, increased TGF receptor-1 density, and increased phosphorylation state of a common transduction convergence point of TGF signaling, Smad-2. Taken together, the results from this study suggest that myocardial expression of MT1-MMP exacerbates post-MI remodeling predominantly through evoking a pro-fibrotic response and, as a consequence, a poor adaptation to a pathological stimulus such as MI.

Although past clinical and animals studies have provided an association between increased myocardial MT1-MMP and adverse LV remodeling (3, 6, 10, 22), this study is the first to directly demonstrate that a common pathological stimulus, such as MI, evokes an early and persistent induction of MT1-MMP at the transcriptional level. Specifically, the present study demonstrated an early induction of MT1-MMP promoter activity within the MI region, which was followed by increased activity within the remote region. These regional and temporal differences in MT1-MMP promoter activity are likely due to the heterogeneous myocardial response, which occurs following MI. Specifically, the MI region undergoes an early inflammatory response, followed by proliferation and expansion of fibroblasts, and ultimately scar formation. This laboratory has reported previously that fibroblasts express MT1-MMP and that this expression is regulated at both the transcriptional and translational level (11). Thus, the early induction of MT1-MMP promoter activity within the MI region is likely due to these early cellular events. Indeed, the present study localized a robust increase in luciferase, indicative of heightened MT1-MMP promoter activity within the interstitial space consistent with fibroblasts. Within the remote region, the viable myocardium undergoes myocyte hypertrophy as well as collagen accumulation, consistent with the remodeling patterns observed in the present study. With longer post-MI periods, the present study demonstrated increased MT1-MMP promoter activity within the remote region, which likely reflects induction within both myocytes and fibroblasts. Concordant with the MT1-MMP promoter studies, steady-state mRNA levels for MT1-MMP were increased at 14 days post-MI. Thus, a likely contributory mechanism for the heightened MT1-MMP abundance and subsequent proteolytic activity that occurred post-MI was due to increased transcription. A past study demonstrated a robust expression of MT1-MMP along the sarcolemmal of human LV myocytes, which was increased in severe LV remodeling and failure (6). The functional and biological significance of the increased and persistent induction of MT1-MMP following MI were next examined in the present study through targeted myocardial overexpression.

In the absence of MI, myocardial MT1-MMPexp caused a mild but demonstrable LV phenotype. Specifically, LV systolic function was reduced and collagen volume fraction was increased; these provided the first evidence that increased myocardial levels of MT1-MMP in and of itself, can modify LV

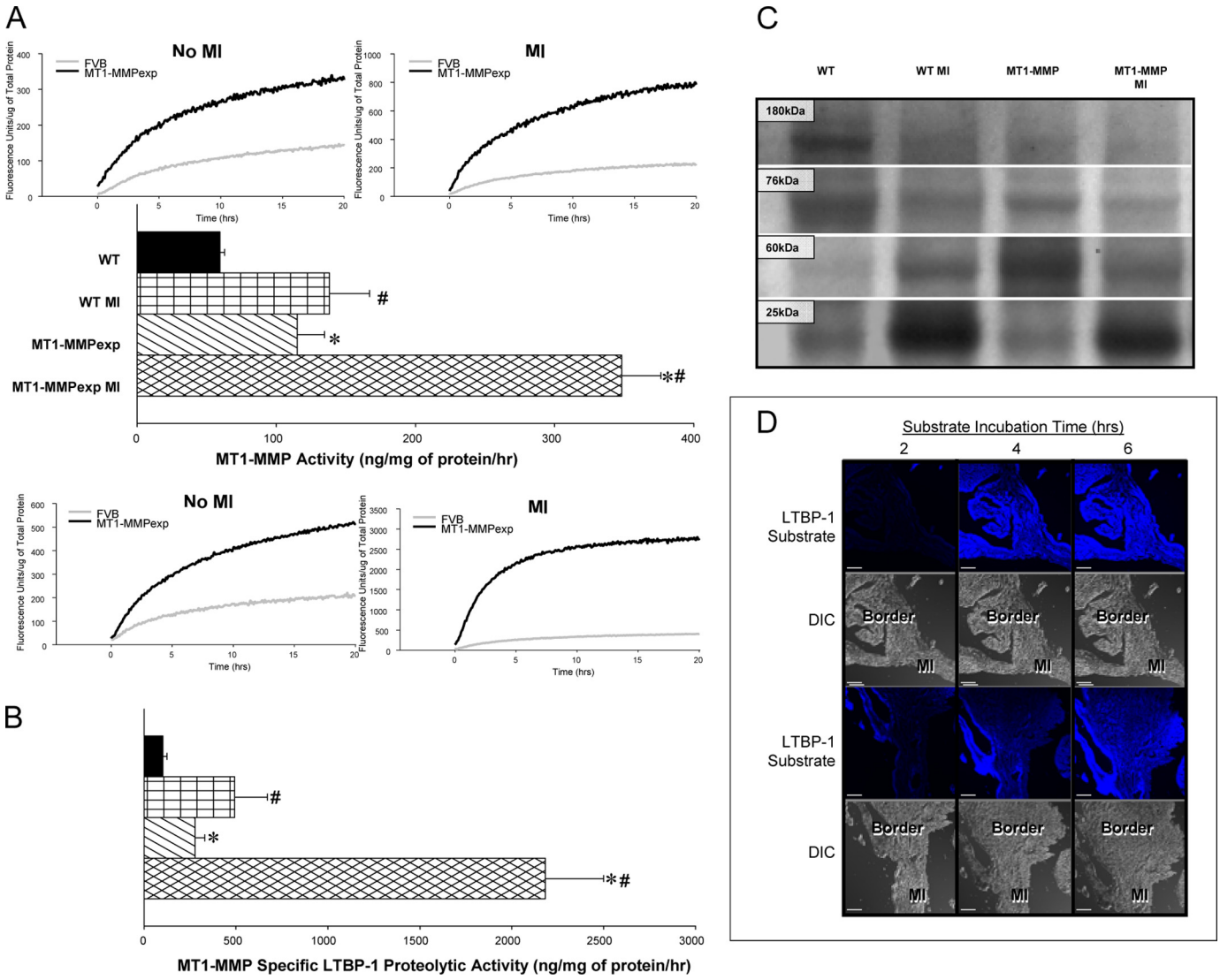

FIGURE 6. *A*, LV myocardial membrane extracts from wild type (*WT*), WT at 14 days post MI, MT1-MMP overexpression (*MT1-MMPexp*), and at 14 days post-MI were utilized to directly measure MT1-MMP catalytic activity ($n = 10$/group) using a calibrated and validated fluorogenic substrate. The membrane/substrate reactions were incubated at 37° C and continuously monitored for specific fluorescence emission, reflective of MT1-MMP proteolytic activity for up to 20 h. Significantly greater MT1-MMP activity occurred in the post-MI *versus* non-MI samples, and therefore the fluorescence values are plotted using different scales. The time-averaged fluorescence (10–20 h) for each sample was determined and using a calibration curve obtained from a recombinant MT1-MMP catalytic domain, actual MT1-MMP activity was computed. Myocardial MT1-MMP activity was increased over respective WT values in the MT1-MMPexp groups. Following MI, MT-MMP activity increased in both groups, but was the highest in the MT1-MMPexp groups ($p = 0.028$, $p = 0.020$, respectively). *B*, the same LV myocardial extracts were then utilized to measure MT1-MMP specific proteolysis using a latency-associated transforming growth factor binding protein-1 (LTBP-1) fluorogenic substrate. Increasing concentrations of MT1-MMP caused a linear increase in LTBP-1 proteolytic activity ($y = 1041x$, $r^2 = 0.99$, $p < 0.001$), which was extinguished with an MT1-MMP-neutralizing antibody. In the LV myocardial extracts, significantly higher MT1-MMP-mediated LTBP-1 proteolytic activity was obtained in the post-MI samples, necessitating the values being plotted using two different scales. Using the MT1-MMP catalytic domain-LTBP-1 fluorescent standard curve, MT1-MMP-mediated LTBP-1 proteolytic activity was computed and was increased in the MT1-MMPexp groups when compared with WT, and was further increased following MI. *C*, LV myocardial membrane extracts were subjected to immunoblotting for LTBP-1. Immunoreactive bands corresponding to the full-length (180 kDa) and proteolytically processed forms of LTBP-1 were observed. Densitometry was performed, and individual LTBP-1 bands normalized to total LTBP-1 levels were computed. A relative reduction in the full-length LTBP-1 was observed in the MT1-MMPexp group compared with WT controls (5.0 ± 0.5 *versus* 3.1 ± 0.7, $\times 10^2$, $p = 0.008$) and fell further in the MT1-MMPexp group following MI (1.1 ± 0.2, $\times 10^2$, $p = 0.001$). In contrast, low molecular weight forms of LTBP-1 increased in the MT1-MMPexp groups. For example, the 60-kDa form of LTBP-1 increased in the MT1-MMPexp group over WT controls (41.6 ± 5.4 *versus* 24.2 ± 2.2, $\times 10^2$, $p = 0.022$). Following MI, the lowest LTBP-1 form was increased in both the WT and MT1-MMPexp groups compared with WT control values (65.0 ± 6.4, 62.6 ± 5.7, *versus* 52.1 ± 3.1, respectively, $\times 10^2$, $p = 0.034$). *D*, to localize MT1-MMP-mediated LTBP-1 proteolytic activity, LV frozen sections were prepared from post-MI WT specimens and incubated with the LTBP-1 fluorogenic substrate and monitored at 37° C for up to 6 h using confocal microscopy. A significant fluorescent signal began to emerge at 2 h following incubation, which occurred to the greatest degree in the border zone and MI regions. Parallel differential interference contrast images are shown below, and these regions are annotated. (*, $p < 0.05$ *versus* WT non-MI; $^+$, *versus* MT1-MMPexp non-MI; $^\#$, $p < 0.05$ *versus* WT MI.)

structure and function. The targeted increase in myocardial MT1-MMP profoundly affected early survival post-MI. There are likely several causes for this observation. First, MT1-MMP is a transmembrane protease and therefore would disrupt critical cell-cell interactions (12–15, 26, 27), which in turn would alter myocardial conduction and increase arrhythmogenesis. Second, MT1-MMP can cause pericellular proteolysis and reduce cellular adhesion to the extracellular matrix (26, 27), which in the context of MI could facilitate myocardial rupture. Third, increased myocardial MT1-MMP levels would likely

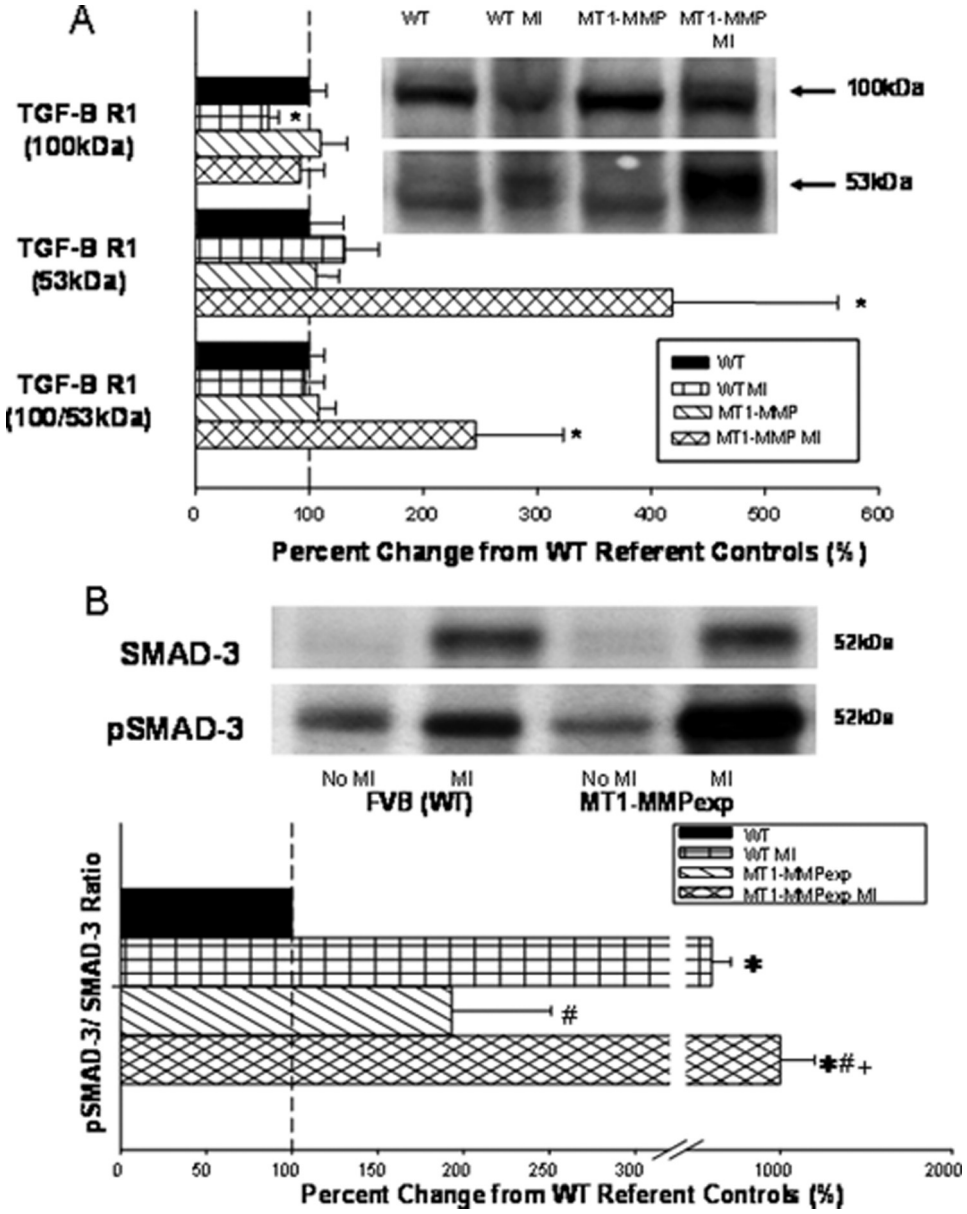

FIGURE 7. *A*, LV myocardial membrane extracts from wild type (*WT*), WT at 14 days post MI, MT1-MMP overexpression (*MT1-MMP*), and at 14 days post-MI ($n = 10$/group) were subjected to immunoblotting for transforming growth factor β receptor-1 (*TGF-BR1*), and the predominant forms were at 53 kDa and a dimer at 100 kDa. The 100-kDa form of TGF-BR1 was reduced in the WT-MI group. TGF-BR1 levels (53 kDa and total) were significantly increased in the MT1-MMP post MI group. *B*, a common Smad, Smad-2 in the classic TGF signaling pathway, was measured in the same LV myocardial extracts in which both total Smad-2 and the phosphorylated form of Smad-2 (*pSmad-2*) were quantified. Total phospho-Smad-2 was increased to the greatest degree in the MT1-MMP post-MI group. (*, $p < 0.05$ *versus* WT non-MI; $^{+}$, *versus* MT1-MMPexp non-MI; $^{\#}$, $p < 0.05$ *versus* WT MI.)

alter the myocyte-matrix interface and thereby diminish the efficiency of LV ejection. In light of the post-mortem studies and the results obtained from the surviving MT1-MMPexp mice, it is likely that all of these factors contributed to reduced post-MI survival. LV dilation is a common structural event following MI and has been well documented to occur in murine models of MI (1–4, 8, 9). In the present study, LV dilation and dysfunction occurred following MI induction in mice, but the degree of LV dysfunction was more severe in the MT1-MMPexp mice. Using an MMP-targeted radiotracer technique (23), the present study demonstrated heightened MMP activity within the MI and remote regions in the MT1-MMPexp mice. This heightened MMP proteolytic activity within the interstitium of the MT1-MMPexp mice likely contributed to further disruption of the myocyte-matrix interface in the early post-MI period, and in turn exacerbated the degree of LV dysfunction. In this relatively early post-MI period, MT1-MMPexp did not appear to cause a greater degree of LV dilation. This may have been due to the fact that those MT1-MMPexp mice with severe LV dilation died during the early post-MI period. Another possible explanation is that the trajectory of LV dilation was similar between the wild-type and MT1-MMPexp mice in this early post-MI period. Another potential mechanism is that the increased matrix accumulation with MT1-MMPexp mechanically impaired LV dilation. Nevertheless, these results clearly demonstrated that MT1-MMPexp directly affected survival and LV function in the early post-MI period.

This is the first study that has directly measured MMP activity through multimodal techniques in the context of MI. It has been demonstrated previously that, once MT1-MMP undergoes translational processing and trafficking to the membrane, then a proteolytically competent enzyme exists (12–15). The extraction and immunoblotting of this transmembrane MMP can result in the identification of several molecular weight forms that can range from 60 to 50 kDa and are likely due to post-translational modification of the cytoplasmic and extracellular domains. Nevertheless, these different molecular weight forms all contain the catalytic domain and therefore retain proteolytic potential. To more carefully address this issue, the present study examined MMP activity, and MT1-MMP proteolytic activity specifically, using several different *in vivo* and *in vitro* approaches. First, using an *in vivo* MMP radiotracer, which binds to the active catalytic domain of all MMP types (23), cardiac restricted MT1-MMPexp resulted in heightened MMP radiotracer binding, which was paralleled by an *ex vivo* measure of total MMP activity using a fluorogenic activity assay (10, 22). Moreover, in the present study, MT1-MMPexp caused a robust increase in

MT1-MMP activity using a specific and previously validated fluorogenic assay (10). These activity assays as well as the immunohistochemical studies confirmed that this MT1-MMPexp transgenic construct yielded overexpression of a functionally competent transmembrane enzyme. In addition, the overall net increase in MMP proteolytic activity, which was demonstrated in the present study, was likely due in large part to increased MT1-MMP-specific induction within the myocardial compartment. More importantly in this MT1-MMPexp construct, *in vivo* and *ex vivo* measurements of MMP/MT1-MMP activity were increased by nearly 2-fold following MI. There are a number of potentially important biological consequences of increased MT1-MMP expression and activity in this early post-MI period. MT1-MMP is an important pathway for proteolytically processing MMP-2 to the active form (12–14). Using a zymographic approach, which provides a sensitive means to identify and size-fractionate MMP-2, higher levels of the active form of MMP-2 were observed in the MT1-MMPexp groups. The emergence of greater amounts of the 68-kDa form would indicate that greater amounts of MMP-2 were processed from the pro-form to the active form. These observations provide the first *in vivo* evidence that selective induction of MT1-MMP within the myocardial compartment in and of itself causes increased levels of an active form of MMP-2. Increased activation of MMP-2 would further contribute to matrix instability and loss of cellular continuity in the MT1-MMPexp mice. Another important consequence of increased myocardial MT1-MMP would be changes at the myocyte-matrix interface. Past *in vitro* studies have demonstrated significant cross-talk between MT1-MMP and transmembrane matrix-binding proteins (integrins) (26, 27) and that MT1-MMP contributes to the phagocytosis of pericellular collagen fragments (26). Finally, and of relevance to the present study, MT1-MMP proteolytically processes a diverse number of biologically active signaling molecules, which in turn would stimulate collagen synthetic pathways (16). Thus, the original concept that MMPs, and in particular that of MT1-MMP, are restricted to degradation of limited set of matrix proteins was likely an oversimplification. In terms of the present study, this would suggest that MT1-MMP induction following MI causes a diverse number of effects that are temporal-, region-, and substrate-dependent.

One of the more unexpected outcomes from these MT1-MMPexp studies was the changes in myocardial collagen content. Total myocardial collagen content was increased by nearly 2-fold with MT1-MMPexp. These findings in and of themselves challenge the canonical belief that myocardial induction of an MMP type, and a resultant increase in net MMP proteolytic activity, will cause an absolute loss in ECM content. The present study directly addressed this issue through a stepwise series of experiments, to determine how increased MT1-MMP myocardial levels may evoke a potent pro-fibrotic response through the TGF pathway. TGF is synthesized as an inactive precursor bound to LTBP-1 through disulfide bonds and a cysteine-rich motif found within LTBP-1 (17, 18). Proteolytic processing of LTBP-1 and subsequent full activation and release of TGF into the interstitium are critical steps in this pro-fibrotic signaling pathway. Through *in silico, in vitro*, and *ex vivo* approaches, the present study provided evidence for a mechanistic link between MT1-MMP proteolytic processing of LTBP-1. First, an MT1-MMP cleavage site for LTBP-1 was identified that falls within a Ca^{2+}-binding EGF-like protein-protein interaction domain of LTBP-1 (residues 1076–1117) (28). Previous studies have identified mutations within a similar type of domain in fibrillin-1, an LTBP-1 homologue, implicated in Marfan syndrome, which results in over-stimulation of TGF signaling (29). Finally, a cell-based assay identified that LTBP-1 may indeed by a proteolytic substrate for MT1-MMP (19). Based upon these observations, a peptide domain of LTBP-1 was then conjugated to a fluorophore to measure specific MT1-MMP proteolytic cleavage of this domain in myocardial extracts. Using this approach, a 2-fold increase in MT1-MMP-specific LTBP-1 proteolysis was demonstrated in the MT1-MMPexp myocardial membranes following MI. In addition, lower molecular weight forms of LTBP-1 suggestive of increased proteolytic processing of LTBP-1 were observed in MT1-MMPexp myocardial extracts. In addition, using this LTBP-1 substrate and *in situ* imaging, specific MT1-MMP-mediated proteolysis could be identified within both the MI and border zone indicating that MT1-MMP-mediated LTBP-1 proteolysis occurred in both the MI region and the viable myocardium. This would imply that increased TGF signaling and a pro-fibrotic response would occur within both the MI scar as well as the viable myocardium. These observations were consistent with the morphometric measurements of collagen content within the LV myocardium using histochemistry. Finally, the present study demonstrated that a robust increase in TGF receptor levels and phosphorylation of a key intracellular signaling component of the TGF pathway Smad2 occurred in the MT1-MMPexp mice following MI. Interestingly, LTBP-1 mRNA levels were reduced in the MT1-MMPexp mice suggestive that alterations in a receptor feedback pathway occurred, which may have been due to heightened TGF signaling in this transgenic construct. While remaining associative, these findings put forth the novel concept that a mechanism for the increased collagen accumulation, which occurred with the induction of myocardial MT1-MMP, is through interstitial proteolysis of LTBP-1, with resultant release of TGF and heightened activation of this potent pro-fibrotic signaling cascade.

Increased myocardial levels of MT1-MMP have been reported previously in the context of LV remodeling in humans and animals (2, 6, 7, 10). The present study utilized a cardiac overexpression model of MT1-MMP, driven by a myosin heavy chain promoter, to induce myocardial MT1-MMP levels to those levels observed in these past studies. However, using the myocyte heavy chain promoter, the preponderance of expression will be restricted to the cardiac myocyte. LV myocardial fibroblasts robustly express MT1-MMP, and increased fibroblast levels of MT1-MMP have been reported in patients with end-stage LV failure (11). Whether MT1-MMP induction in fibroblasts as well as in cardiac myocytes may cause a more severe LV phenotype remains to be explored. In addition, using this human MT1-MMP overexpression construct, endogenous mouse MT1-MMP levels were reduced, suggestive of compensatory feedback in MT1-MMP expression, which highlights potential limitations to a transgenic overexpression model. The

present study examined the consequences of MT1-MMP overexpression, but targeted down-regulation of this MMP was not addressed. Past studies have demonstrated that MT1-MMP gene deletion is associated with significant developmental malformations (30), and therefore utilizing a global deletion model would be problematic. Moreover, global MMP inhibition, which would putatively inhibit MT1-MMP has been performed previously (4, 7, 9). However, these nonselective MMP inhibition strategies are difficult to actuate clinically (25). Thus, based upon past studies identifying increased MT1-MMP levels in the failing human myocardium (6), and the results from the present study, more targeted and selective transgenic/pharmacological strategies to selectively interrupt MT1-MMP myocardial expression and activity in the context of LV remodeling would be warranted.

Acknowledgments—We thank Dr. Jeffrey Jones, Medical University of South Carolina, for his assistance with the time-lapse confocal studies, and Drs. David H. Lovett and Rajeev Mahimkar, University of California at San Francisco, for assistance with the MT1-MMP reporter construct.

REFERENCES

1. Sundström, J., Evans, J. C., Benjamin, E. J., Levy, D., Larson, M. G., Sawyer, D. B., Siwik, D. A., Colucci, W. S., Sutherland, P., Wilson, P. W., and Vasan, R. S. (2002) *Circulation* **109,** 2850–2856
2. Vanhoutte, D., Schellings, M., Pinto, Y., and Heymans, S. (2006) *Cardiovasc. Res.* **69,** 604–613
3. Wilson, E. M., Moainie, S. L., Baskin, J. M., Lowry, A. S., Deschamps, A. M., Mukherjee, R., Guy, T. S., St John-Sutton, M. G., Gorman, J. H., 3rd, Edmunds, L. H., Jr., Gorman, R. C., and Spinale, F. G. (2003) *Circulation* **107,** 2857–2863
4. Heymans, S., Luttun, A., Nuyens, D., Theilmeier, G., Creemers, E., Moons, L., Dyspersin, G. D., Cleutjens, J. P., Shipley, M., Angellilo, A., Levi, M., Nübe, O., Baker, A., Keshet, E., Lupu, F., Herbert, J. M., Smits, J. F., Shapiro, S. D., Baes, M., Borgers, M., Collen, D., Daemen, M. J., and Carmeliet, P. (1999) *Nat. Med.* **5,** 1135–1142
5. Spinale, F. G., Coker, M. L., Thomas, C. V., Walker, J. D., Mukherjee, R., and Hebbar, L. (1998) *Circ. Res.* **82,** 482–495
6. Spinale, F. G., Coker, M. L., Heung, L. J., Bond, B. R., Gunasinghe, H. R., Etoh, T., Goldberg, A. T., Zellner, J. L., and Crumbley, A. J. (2000) *Circulation* **102,** 1944–1949
7. King, M. K., Coker, M. L., Goldberg, A., McElmurray, J. H., 3rd, Gunasinghe, H. R., Mukherjee, R., Zile, M. R., O'Neill, T. P., and Spinale, F. G. (2003) *Circ. Res.* **92,** 177–185
8. Matsusaka, H., Ide, T., Matsushima, S., Ikeuchi, M., Kubota, T., Sunagawa, K., Kinugawa, S., and Tsutsui, H. (2006) *Hypertension* **47,** 711–717
9. Ikonomidis, J. S., Hendrick, J. W., Parkhurst, A. M., Herron, A. R., Escobar, P. G., Dowdy, K. B., Stroud, R. E., Hapke, E., Zile, M. R., and Spinale, F. G. (2005) *Am. J. Physiol. Heart Circ Physiol* **288,** H149–H158
10. Deschamps, A. M., Yarbrough, W. M., Squires, C. E., Allen, R. A., McClister, D. M., Dowdy, K. B., McLean, J. E., Mingoia, J. T., Sample, J. A., Mukherjee, R., and Spinale, F. G. (2005) *Circulation* **111,** 1166–1174
11. Spruill, L. S., Lowry, A. S., Stroud, R. E., Squires, C. E., Mains, I. M., Flack, E. C., Beck, C., Ikonomidis, J. S., Crumbley, A. J., McDermott, P. J., and Spinale, F. G. (2007) *Am. J. Physiol.* **293,** C1362–C1373
12. Guo, C., and Piacentini, L. (2003) *J. Biol. Chem.* **278,** 46699–46708
13. Strongin, A. Y., Collier, I., Bannikov, G., Marmer, B. L., Grant, G. A., and Goldberg, G. I. (1995) *J. Biol. Chem.* **270,** 5331–5338
14. Okada, A., Tomasetto, C., Lutz, Y., Bellocq, J. P., Rio, M. C., and Basset, P. (1997) *J. Cell Biol.* **137,** 67–77
15. Sodek, K. L., Ringuette, M. J., and Brown, T. J. (2007) *Br. J. Cancer* **97,** 358–367
16. Tam, E. M., Morrison, C. J., Wu, Y. I., Stack, M. S., and Overall, C. M. (2004) *Proc. Natl. Acad. Sci. U.S.A.* **101,** 6917–6922
17. Ruiz-Ortega, M., Rodríguez-Vita, J., Sanchez-Lopez, E., Carvajal, G., and Egido, J. (2007) *Cardiovasc. Res.* **74,** 196–206
18. Bujak, M., and Frangogiannis, N. G. (2007) *Cardiovasc. Res.* **74,** 184–195
19. Tatti, O., Vehviläinen, P., Lehti, K., and Keski-Oja, J. (2008) *Exp. Cell Res.* **314,** 2501–2514
20. Gulick, J., Subramaniam, A., Neumann, J., and Robbins, J. (1991) *J. Biol. Chem.* **266,** 9180–9185
21. Mukherjee, R., Mingoia, J. T., Bruce, J. A., Austin, J. S., Stroud, R. E., Escobar, G. P., McClister, D. M., Jr., Allen, C. M., Alfonso-Jaume, M. A., Fini, M. E., Lovett, D. H., and Spinale, F. G. (2006) *Am. J. Physiol. Heart Circ. Physiol.* **291,** H2216–H2228
22. Spinale, F. G., Escobar, G. P., Mukherjee, R., Zavadzkas, J. A., Saunders, S. M., Jeffords, L. B., Leone, A. M., Beck, C., Bouges, S., and Stroud, R. E. (2009) *Circ. Heart Fail.* **2,** 351–360
23. Su, H., Spinale, F. G., Dobrucki, L. W., Song, J., Hua, J., Sweterlitsch, S., Dione, D. P., Cavaliere, P., Chow, C., Bourke, B. N., Hu, X. Y., Azure, M., Yalamanchili, P., Liu, R., Cheesman, E. H., Robinson, S., Edwards, D. S., and Sinusas, A. J. (2005) *Circulation* **112,** 3157–3167
24. Kridel, S. J., Sawai, H., Ratnikov, B. I., Chen, E. I., Li, W., Godzik, A., Strongin, A. Y., and Smith, J. W. (2002) *J. Biol. Chem.* **277,** 23788–23793
25. Holmbeck, K., Bianco, P., Caterina, J., Yamada, S., Kromer, M., Kuznetsov, S. A., Mankani, M., Robey, P. G., Poole, A. R., Pidoux, I., Ward, J. M., and Birkedal-Hansen, H. (1999) *Cell* **99,** 81–92
26. Barbolina, M. V., and Stack, M. S. (2008) *Semin. Cell Dev. Biol.* **19,** 24–33
27. Baciu, P. C., Suleiman, E. A., Deryugina, E. I., and Strongin, A. Y. (2003) *Exp. Cell Res.* **291,** 167–175
28. Koli, K., Saharinen, J., Hyytiäinen, M., Penttinen, C., and Keski-Oja, J. (2001) *Microsc. Res. Tech.* **52,** 354–362
29. Neptune, E. R., Frischmeyer, P. A., Arking, D. E., Myers, L., Bunton, T. E., Gayraud, B., Ramirez, F., Sakai, L. Y., and Dietz, H. C. (2003) *Nat. Genet.* **33,** 407–411
30. Peterson, J. T. (2006) *Cardiovasc. Res.* **69,** 677–687